Icarus 252 (2015) 22–31

Contents lists available at ScienceDirect

Icarus

journal homepage: www.elsevier.com/locate/icarus

Meteoroid impacts onto asteroids: A competitor for Yarkovsky and YORP

Paul A. Wiegert *

Department of Physics and Astronomy, The University of Western Ontario, London, Canada
Center for Planetary Science and Exploration, The University of Western Ontario, London, Canada

ARTICLE INFO

Article history:
Received 14 July 2014
Revised 2 December 2014
Accepted 18 December 2014
Available online 8 January 2015

Keywords:
Near-Earth objects
Asteroids, dynamics
Asteroids, rotation
Celestial mechanics
Impact processes
Meteorites
Meteors

ABSTRACT

The impact of a meteoroid onto an asteroid transfers linear and angular momentum to the larger body, which may affect its orbit and its rotational state. Here we show that the meteoroid environment of our Solar System can have an effect on small asteroids that is comparable to the Yarkovsky and Yarkovsky–O'Keefe–Radzievskii–Paddack (YORP) effects under certain conditions.

The momentum content of the meteoroids themselves is expected to generate an effect much smaller than that of the Yarkovsky effect. However, momentum transport by ejecta may increase the net effective force by one order of magnitude for iron or regolith surfaces, and two orders of magnitude for impacts into bare rock surfaces. The result is sensitive to the extrapolation of laboratory microcratering experiment results to real meteoroid-asteroid collisions and needs further study. If this extrapolation holds, then meteoroid impacts are more important to the dynamics of small rocky asteroids than had previously been considered.

Asteroids orbiting on prograde orbits near the Earth encounter an anisotropic meteoroid environment, including a population of particles on retrograde orbits generally accepted to be material from long-period comets spiralling inwards under Poynting–Robertson drag. High relative speed (60 km s^{-1}) impacts by meteoroids provide a small effective drag force that decreases asteroid semimajor axes and which is independent of their rotation pole. If small asteroids are bare instead of regolith covered, as is perhaps to be expected given their rapid rotation rates (Harris, A.W., Pravec, P. [2006]. In: Daniela, L., Sylvio Ferraz, M., Angel, F.J. (Eds.), Asteroids, Comets, Meteors. IAU Symposium, vol. 229, pp. 439–447), this effect may exceed the instantaneous Yarkovsky drift at sizes near and below one meter. Since one meter objects are the most abundant meteorite droppers at the Earth, the delivery of these important objects may be controlled by drag against the meteoroid environment.

The rate of reorientation of asteroid spins is also substantially increased when momentum transport by ejecta is included. This has an indirect effect on the net Yarkovsky drift, particularly the diurnal variant, as the sign of the drift it creates depends on its rotational state. The net drift of an asteroid towards a resonance under the diurnal Yarkovsky effect can be slowed by more frequent pole reorientations or induced tumbling. This may make the effect of the meteoroid environment more important than the Yarkovsky effect at sizes even above one meter.

Meteoroid impacts also affect asteroid spins at a level comparable to that of YORP at sizes smaller than tens of meters. Here the effect comes primarily from a small number of impacts by centimeter size particles. We conclude that recent measurements of the YORP effect have probably not been compromised, because of the targets' large sizes and because they are known or likely to be regolith-covered rather than bare rock. However, the effect of impacts increases sharply with decreasing size, and will likely become important for asteroids smaller than a few tens of meters in radius.

1. Introduction

The study of the delivery of meteorites to Earth was much advanced by the revival of the notion that the uneven re-radiation of incident sunlight could affect the orbits of small asteroids. Known as the Yarkovsky effect, this phenomenon results when temperature differences on an asteroid's surface result in it reradiating energy (and hence momentum) asymmetrically. The Yarkovsky effect has been widely discussed elsewhere (the reader is directed to Rubincam (1998) and Farinella et al. (1998) for excellent reviews). It is of interest here because it is one of few dynamical effects acting in the main asteroid belt which create a

* Address: Department of Physics and Astronomy, The University of Western Ontario, London, Canada. Fax: +1 519 661 2033.
E-mail address: pwiegert@uwo.ca

http://dx.doi.org/10.1016/j.icarus.2014.12.022
0019-1035/

net trend in the semimajor axis a of an asteroid's orbit. If such a change in a moves the body into a mean-motion or other resonance, its orbit may be dramatically changed as a result. Resonances can eject asteroids from the asteroid belt and play a key role in the delivery of meteorites to Earth. Thus the Yarkovsky effect, while itself creating only a small change in asteroid orbits, is nonetheless crucial in moving meteorite parent bodies from the asteroid belt to near-Earth space. The importance of the Yarkovsky effect leads one to consider whether or not other small effects might have important roles in the evolution of small asteroids. Here we consider the effect of momentum transfer via meteoroid impacts and show that it can compete with the Yarkovsky effect (and its cousin, the Yarkovsky–O'Keefe–Radzievskii–Paddack or YORP effect) under certain conditions.

In Section 2 we will introduce the meteoroid environment near the Earth. In Section 3, the dynamical effects of meteoroid impacts on small asteroids, and in particular the role of momentum transport by ejecta, will be discussed and comparisons drawn with the Yarkovsky effect. Section 4 extends the discussion to the YORP effect, Section 5 considers radiation pressure and rates of erosion and conclusions are drawn in Section 6.

2. Meteoroid environment at Earth

Most of the mass accreted by the Earth is in small particles, at least over short times. Larger individual asteroid impacts may dominate the overall mass input to the Earth (Rabinowitz, 1993; Rabinowitz et al., 1993) on million year timescales but they are not relevant here. Love and Brownlee (1993) determined that meteoroids with mass $m \approx 1.5 \times 10^{-8}$ kg corresponding to a radius $r = 220$ μm at a density $\rho_p = 2500$ kg m^{-3} dominate the meteoroid flux at Earth. Earlier studies such as those of Grün et al. (1985) found similar values though with total fluxes somewhat (2–3 times) lower.

At these sizes, the meteoroid environment of the Earth is asymmetric. This is partly because of the Earth's motion around the Sun: our planet tends to get hit more on the leading side than the trailing side. However the asymmetry also originates in part from a heterogeneous distribution of particle orbits. Studies of the *sporadic* meteors (that is, those meteors distinct from *meteor showers*) show concentrations of meteoroid orbits towards the direction of the Earth's motion around the Sun (e.g. Stohl, 1986; Brown and Jones, 1995; Chau et al., 2007; Campbell-Brown, 2008) and many others). When displayed in a co-moving reference frame centered on the apex of the Earth's way, a number of concentrations of impinging orbits are discerned. Here we will be most interested in those known as the north and south apex sporadic meteor sources.

Meteoroids arriving at Earth from these apex sources have relative velocities peaking at 60 km s^{-1} (Jones and Brown, 1993; Chau et al., 2007). These particles are on approximately circular retrograde orbits. Attributed to long-period and Halley-family cometary debris that has decayed onto low-eccentricity orbits through Poynting–Robertson drag, these particles constitute the dominant momentum and kinetic energy flux in near-Earth space. Because they arrive from the direction of the Earth's motion, they hit our planet essentially head-on and provide a small but consistent tangential drag force on any body (such as an asteroid) on a similar orbit. Though the meteoroid environment at the asteroid belt is not well known, it is reasonable to assume that it is similar to that at Earth and will also produce a net drag on asteroidal bodies.

The fraction of retrograde meteoroids arriving at Earth has been measured but there are still uncertainties. Radial scatter meteor radars (often called "High Power Large Aperture" or HPLA radars) typically see a larger fraction of apex meteors (>80%) (e.g. Sato et al., 2000; Hunt et al., 2004; Janches et al., 2003; Chau and Woodman, 2004) while transverse scatter (or "meteor patrol") radars, typically see a smaller fraction (~50%) (e.g. Taylor, 1995; Galligan and Baggaley, 2004) as do video meteor systems (Campbell-Brown and Braid, 2011). This effect can be attributed to the different instrumental sensitivities (Wiegert et al., 2009) at different particle sizes and speeds; however here for simplicity we will assume that the apex meteoroids constitute a fraction $s = 50\%$ of the meteoroid population at these sizes. The magnitude of the effect of this idealized meteoroid environment on a target asteroid will be calculated first at Earth. For simplicity we will ignore the helion and anti-helion sources, whose strengths are similar to each other and whose impact effects tend to cancel each other out. The meteoroid complex as a whole should be considered carefully in a more detailed study but this is beyond the scope of this work, where we simply show the order of magnitude of the effects.

If the meteoroid flux at the Earth is dominated by the apex source as studies of the sporadic meteors would suggest, then taking the (cumulative) flux from Fig. 3 of Love and Brownlee (1993), where their differential flux peaks ($m \approx 1.5 \times 10^{-8}$ kg) we get $n \approx 3 \times 10^{-8}$ m^{-2} s^{-1} where n is the flux of particles per square meter per second, and m is the particle mass. Given these conditions, a one-meter radius asteroid on a circular orbit near the Earth sees roughly three impacts per year, and each of impactor carries ~10^{-12} of the momentum of the target. We will consider their cumulative effect to be a small effective drag on the target asteroid.

3. Effective drag due to meteoroid impacts

The impact of a small meteoroid onto an asteroid surface transfers kinetic energy and momentum to the larger body. Using the impulse approximation, the force F exerted on the asteroid as a result of a momentum gain Δp during a time Δt is $F = \Delta p/\Delta t$. The fraction η of the incoming momentum received by the target is unity in the case of a completely inelastic collision, and could be as high as two in the case of an elastic collision. However, high-velocity impacts are highly inelastic and we will adopt $\eta \approx 1$.

The acceleration $f_a = F/M$ imparted to an assumed spherical asteroid of mass M, density ρ_a and radius R being impacted head-on by the apex meteoroid population as described earlier would be

$$f_a = \frac{snm v \pi R^2}{\frac{4}{3}\pi \rho_a R^3} = \frac{3snm v}{4R\rho_a} \tag{1}$$

where v is the relative velocity.

Lagrange's planetary equations e.g. Roy (1978) can be used to calculate the resulting change in semimajor axis a for an asteroid with zero eccentricity and inclination that is subject to a tangential acceleration such as that of Eq. (1)

$$\dot{a} \approx -\frac{2f_a}{n'} = -\frac{3snm v a^{3/2}}{2\sqrt{GM_\odot} R \rho_a} \tag{2}$$

where $n' = \sqrt{GM_\odot/a^3}$ is the asteroid's mean motion. For an $R = 1$ m target asteroid at 1 AU, the apex meteoroid environment produces a decrease in semimajor axis of

$$\dot{a} \approx -6.1 \times 10^{-6} \left(\frac{s}{0.5}\right) \left(\frac{R}{1\text{ m}}\right)^{-1} \left(\frac{\rho_a}{3500\text{ kg m}^{-3}}\right)^{-1} \text{AU Myr}^{-1} \tag{3}$$

This effective drag force is much lower than that of the Yarkovsky effect in its different variants, by factors of several up to 100 (e.g. Fig. 1 of Farinella et al. (1998)).

Though direct momentum transfer as described above may be negligible compared to the Yarkovsky effect, there are two subsidiary effects that may make small asteroids' interactions with the meteoroid environment important. First, we will show that the ejecta produced by the impact results in a much larger momentum transfer to the target than simply that carried by the impactor, magnifying the effective force. Secondly, this may also shorten the timescale between collisional re-orientation of the asteroid's spin axis, an important consideration for the Yarkovsky effect, particularly the diurnal variant.

3.1. Momentum transport by ejecta

A hypervelocity impact creates a crater on the target, and the amount of mass removed during this process is often larger than the mass of the projectile itself. The incoming particle is vapourized on impact since its kinetic energy content vastly exceeds its internal binding energy, and the resulting explosive event excavates a crater in the target. Consider the impact as seen in the reference frame of the center of mass of the impactor-target pair. Taking the impactor's mass to be m and its impact velocity v, a fraction ϵ of the impactor's kinetic is converted to kinetic energy of motion of the ejecta and target, resulting the ejection of a mass Nm of target material at a velocity γv, where N and γ are multiplicative factors that depend on the detailed physics of impact.

After the impact, the ejecta carries away momentum γNmv which by Newton's Third Law is balanced by an opposite momentum transfer to the target. The ratio of the momentum of the ejecta to that of the projectile itself $N\gamma$ can exceed unity. The ratio of the momentum transferred to the target relative to that of the impactor is called the 'momentum multiplication factor' β (e.g. Housen and Holsapple, 2011) and so we have $\beta = 1 + N\gamma$. Since $\beta > 1$, then the mobilization of ejecta creates an effective force that exceeds that due simply to the momentum content of the projectile. Note that $\beta > 1$ does not violate conservation of momentum. The kinetic energy of the impactor provides energy for the release of ejecta, and it is conservation of momentum between the ejecta and the target that provide the effective force that we consider here.

The value of β can be related to ϵ, N and γ. Our definition of ϵ implies that

$$\frac{1}{2}\epsilon m v^2 = \frac{1}{2}Nm(\gamma v)^2 + \frac{1}{2}MV^2 \tag{4}$$

where M is the mass of the target after impact, and V its speed. The ratio of the kinetic energy acquired by the target to that of the ejecta is

$$\frac{\frac{1}{2}MV^2}{\frac{1}{2}Nm(\gamma v)^2} = \frac{MV^2}{Nm(\gamma v)^2} \tag{5}$$

Conservation of momentum implies that

$$(Nm)(\gamma v) = MV \tag{6}$$

$$V = \frac{\gamma Nmv}{M} \tag{7}$$

which when substituted back into Eq. (5) gives

$$\frac{MV^2}{Nm(\gamma v)^2} = \frac{M\left(\frac{\gamma Nmv}{M}\right)^2}{Nm(\gamma v)^2} \tag{8}$$

$$= \frac{Nm}{M} \tag{9}$$

The target carries only a fraction Nm/M of the kinetic energy which is negligible in the limit that the target mass is much larger than the amount of mass released by the impact. Since this applies to most of the impacts we consider here, this allows us to simplify Eq. (4) to

$$\frac{1}{2}\epsilon m v^2 \approx \frac{1}{2}Nm(\gamma v)^2 \tag{10}$$

$$\epsilon \approx N\gamma^2 \tag{11}$$

From this, we obtain $\gamma \approx \sqrt{\epsilon/N}$ and

$$\beta = N\gamma \approx \sqrt{\epsilon N} \tag{12}$$

We will see below that for typical microcratering events expected on asteroids, N is very large ($\gtrsim 10^4$) and $\beta \sim 100$, which pushes the resulting drag force into a range comparable to that of the Yarkovsky effect for small asteroids. This is a linchpin argument of this paper, namely that momentum transport by ejecta creates a substantially larger effective force on the target than if the simple momentum content of the projectile would imply. Since hypervelocity cratering is complex, our analysis may be over-simplified and further study by experts in that field is greatly encouraged by this author.

3.2. Microcratering experiments

Microcratering experiments involve accelerating of particles to high speeds in the lab and directing them onto targets composed of the materials of interest. Such experiments often measure the amount of material excavated (N), while the values for ejecta velocities (γ) and energies (ϵ) are less well-studied. We will use experimental measures of N and ϵ, seeming to be the best constrained of the three, to estimate γ and show that our value of γ is consistent with those experiments that have measured ejecta velocities.

Here we consider the same target cases as Farinella et al. (1998) who provide a very clear exposition of the effects of the Yarkovsky effect on meter-class asteroids of various types. We assume our target asteroids are either bare rock, regolith-covered rock or bare iron. Bare or regolith-covered rock are the best studied in terms of microcratering experiments, having received much attention during the Apollo era (e.g. Fechtig et al., 1972).

Bare rock surfaces are perhaps more likely for small asteroids, which tend to spin above the spin-barrier (Harris and Pravec, 2006). In Hatch and Wiegert (2015) the near-Earth asteroids below 60 m in size with well-determined periods are found to rotate on average once per 40 min, well below the spin-barrier of ~2.2 h. Thus we expect that bare rock is the relevant scenario for the smallest asteroids.

Gault (1973) provides empirically-based formulae for the displaced mass as a function of the kinetic energy. After firing a variety of projectiles (densities of 0.95–7.8 g cm^{-3}) into a selection of terrestrial rocks (including basalt) as well as the Indarch meteorite (range of target densities: 2.5–5 g cm^{-3}) at high-velocity and normal incidence, the mass displaced M_e in grams was found to be

$$M_e = 10^{-10.061}\left(\frac{\rho_p}{\rho_a}\right)^{1/2}(KE)^{1.133} \tag{13}$$

where ρ_p is the projectile density (g cm^{-3}), ρ_a is the target density (g cm^{-3}) and KE is the kinetic energy in ergs. Gault's formula is applicable to craters with diameters from 10^{-3} to 10^3 cm with impact kinetic energies of 10—10^{12} ergs. An impact by a 1.5×10^{-8} kg particle at 60 km s^{-1} has an energy of 2.7×10^8 ergs and falls squarely in this range. The resulting $N = M_e/m$ is

$$N \approx 2.1 \times 10^4\left(\frac{\rho_p}{\rho_a}\right)^{1/2}\left(\frac{m}{1.5\times10^{-8}\,\mathrm{kg}}\right)^{0.133}\left(\frac{v}{6\times10^4\,\mathrm{m\,s^{-1}}}\right)^{2.266} \tag{14}$$

A hypervelocity impact can displace four orders of magnitude more mass than that of the projectile. For the case of dense minerals and

glass, microcratering is often accompanied by large spalled regions, annuli around the crater itself where material fractures off in large plates or flakes (e.g. Hörz et al., 1971) and this contributes to the relatively large mass displaced.

The fraction of impactor kinetic energy that goes into the motion of the ejecta has been found experimentally to be small for low impact speeds but to increase sharply as speed increases. Braslau (1970) found $\epsilon \approx 0.5$ both for dry quartz sand and basalt at impact speeds of 6 km s^{-1}. Later studies by Hartmann (1983) were somewhat critical of Braslau's assumptions but still found $\epsilon \approx 0.3$ as the impact speed increased to 4 km s^{-1}. Here we will adopt $\epsilon = 0.5$ since we are considering even higher speeds, while noting that our expression for β is relatively insensitive to its precise value, going only like $\epsilon^{1/2}$ (Eq. (12)).

Together with Eqs. (11) and (14) this allows us to estimate $\gamma \approx \sqrt{\epsilon/N} \approx 5 \times 10^{-3}$. This value, which implies ejecta velocities around 0.3 km s^{-1} for a 60 km s^{-1} impact, is consistent with experimental measurements of late-stage ejecta from loose sand targets (Braslau, 1970) and powdered targets of pumice and basalt (Hartmann, 1985), though the ejecta were found to have a wide range of velocities.

From the values for ϵ and N, we deduce an $\beta \approx \sqrt{\epsilon N} \approx 10^2$ (from Eq. (12)) for bare rock: the cratering process can release two orders of magnitude more momentum than is carried by the projectile itself. As a result, Eq. (3) should be multiplied by a factor $\beta \sim 100$, which makes it competitive with the Yarkovsky effect under some conditions (this will be discussed in more detail in Section 3.3).

A few modern experiments have measured the transfer of momentum directly to the target. These experiments have been done at speeds below that of the meteoroid impacts discussed above but can be extrapolated to higher speeds. Housen and Holsapple (2012) report that rocky targets impacted by polyethylene, aluminum or nylon impactors have β that scales as v; they report $\beta \sim 20$ at 30 km s^{-1} which scales to ~40 at 60 km s^{-1}. Yanagisawa and Hasegawa (2000) find β (their η) ~2.5 at near-normal impact of nylon projectiles into basalt at 4 km s^{-1}, which scaled like v gives $\beta \sim 38$ at 60 km s^{-1}. Tedeschi et al. (1995) report 'unexpectedly large measured values of momentum enhancement to some of the targets' with aluminum impactors into rocky targets. They could only set upper limits for most rocky targets, with $3 \lesssim \beta \lesssim 10$ at 8 km s^{-1} (scaling with v implies $23 \lesssim \beta \lesssim 75$ at 60 km s^{-1}). These values imply a β somewhat lower than that derived from Gault (1973): we again note that all of these results are based on an extrapolation of microcratering results beyond the impact speeds actually examined in the lab, and a more detailed examination of the phenomenon is certainly warranted.

Larger asteroids are likely to be regolith-covered. Spacecraft missions to near-Earth asteroids (NEAs) such as (433) Eros (Cheng, 2002) and (25143) Itokawa (Saito et al., 2006) show surfaces covered with fine particulates. Radar studies of 7 km diameter NEA (53319) 1999 JM_8 reveal regolith cover (Carter et al., 2006). Infrared studies of NEAs reveal the regolith-free bodies may be uncommon even down to sizes of a few hundred meters (Delbó et al., 2003). Impacts into mineral dust, which would be more applicable to regolith-covered bodies, produce similar results to bare rock though the displaced masses are often lower. High-velocity impacts by centimeter sized particles displace two to four orders of magnitude more mass than that of the projectile (references in Vedder (1972) incl. Braslau (1970)) with loosely-packed material being more easily displaced than packed or consolidated material. For 2 to 5 μm-sized polystyrene (1.06 g cm^{-3}) spheres accelerated to 2.5 to 12 km s^{-1} into mineral dust, the amount of displaced mass was three orders of magnitude larger than the impactor mass, though the granular nature of the target resulted in large (±50%) uncertainties in displaced mass. For impacts into granular material, we conclude that N may be lower, reducing β. Since small meteorite parent bodies are expected to be bare rock, we will adopt $\beta = 100$ here as our fiducial value for stony targets, recognizing that it may be smaller if the targets are actually covered with regolith.

For the case of bare iron, Comerford (1967) found that 2.6 km s^{-1} silicon carbide particles eroded the Hoba iron meteorite at least two orders of magnitude more slowly than the Indarch chondrite meteorite, implying $N \lesssim 200$ from simple extension of Eq. (14). Schaeffer et al. (1979) fired 1.5—2 mm steel and sapphire particles into the Gibeon iron meteorite and also found that plastic flow significantly reduced the amount of material released. They concluded that the erosion rate of iron meteorites was a factor of 10 slower than that of stony ones ($N \sim 2000$).

Comerford (1967) points out that much depends here on the brittle versus ductile nature of the target, which is sensitive to crystal size and temperature. Higher velocity impacts at the lower temperatures of the asteroid belt may move into the brittle fracture (instead of the ductile flow) regime which may release more ejecta. However it seems unlikely that N values approaching those of rock targets would be reached. If we adopt the values of $N \sim 200$ and take $\epsilon = 0.5$ as before, we have $\beta = 10$ for iron meteorite parents, recognizing it contains a substantial uncertainty. Nonetheless, even on iron targets, it seems that significantly more momentum may be carried by the ejecta than is received from the impinging particle.

If ejecta do generally carry away 10–100 times as much momentum as is imparted by the meteoroid, then Eq. (3) is 10–100 times higher, and becomes competitive with the Yarkovsky effect. Before comparing them side-by-side, let us first extrapolate the near-Earth meteoroid environment to the asteroid belt.

3.3. Extrapolation to the asteroid belt

Eq. (3) assumes a meteoroid environment like that at Earth. If we are interested in whether or not impact drag competes with the Yarkovsky effect in the delivery of small asteroids to resonance 'escape hatches' in the asteroid belt, we need to consider the meteoroid environment there. Unfortunately, there is little experimental data on the asteroid belt's meteoroid environment. Here we simply assume that the environment at Earth has evolved directly from that at the asteroid belt under Poynting–Robertson (PR) drag.

The apex meteoroids encountered by our planet are on roughly circular retrograde orbits (Jones and Brown, 1993; Chau et al., 2007), and thought to be particles released from retrograde comets whose semimajor axis a and eccentricity e have decayed through Poynting–Robertson drag. We assume here that the asteroid belt hosts the same meteoroids (at an earlier time) as they spiral inwards to produce the meteoroids observed at Earth, and that we can estimate the properties of the asteroid belt meteoroid environment from meteor observations taken here.

Returning to Eq. (2), let us assume that the impactor mass m, the target radius R and density ρ_a are not functions of heliocentric distance. The factors that are include the velocity of each impact v, which goes like $a^{-1/2}$ owing to Kepler's Third Law. The flux of impactors n is also affected: it is proportional to v times the number density of particles n_p. Assuming the meteoroids are spiralling inwards under PR drag near the ecliptic plane, the vertical and azimuthal densities of particles both go like a^{-1} while the radial density is proportional to $1/\dot{a}_{PR}$, where $\dot{a}_{PR}$ is the rate at which the meteoroids spiral inwards under PR drag. The effect of PR drag on particle semimajor axis is given by Weidenschilling and Jackson (1993) to be $\dot{a}_{PR} \propto a^{-1}$ for circular orbits. This result of these factors is that $n_p \propto a^{-1}$, and the flux $n = v n_p \propto a^{-3/2}$. Eq. (2) would increase like $a^{3/2}$ if n and v were constant, but $\dot{a}$ will instead decrease slightly (as $a^{-1/2}$) with increasing semimajor axis.

When extended to the distance of the main asteroid belt, Eq. (3) becomes

$$\dot{a} = -4.3\times10^{-4}\left(\frac{s}{0.5}\right)\left(\frac{\beta}{100}\right)\left(\frac{a}{2\,\mathrm{AU}}\right)^{-1/2}\left(\frac{R}{1\,\mathrm{m}}\right)^{-1}\left(\frac{\rho_a}{3500\,\mathrm{kg\,m^{-3}}}\right)^{-1}\mathrm{AU\,Myr^{-1}} \quad (15)$$

Eq. (15) is expressed at the same heliocentric semimajor axis (2 AU) considered by Farinella et al. (1998) in their analysis of the Yarkovsky effect, which allows us to compare our results directly with theirs.

For bare rock (Fig. 1) impact drag exceeds two of the three variants of the Yarkovsky effect considered by Farinella et al. (1998) (the seasonal effect and the diurnal effect under the assumption of size-dependent spin) but only at sizes of tens of centimeters. The drag effect considered here is smaller than the diurnal effect in the case where the spins of small asteroids are independent of their sizes, though Farinella et al. (1998) indicate that size dependent spin states are more realistic in their opinion. If Farinella et al. (1998) are right and spin rates are typically higher for smaller asteroids, then the effect presented here is of the same order of magnitude as the Yarkovsky effect for meter class asteroids, while the seasonal effect dominates at larger sizes.

For bare iron asteroids (Fig. 2) meteoroid drag is less effective, though it could still exceed the Yarkovsky effect at small target sizes if 60 km s^{-1} impacts take place in the brittle rather than ductile deformation regimes (that is, if β is larger than assumed here). In Fig. 2, we account for the increased density of the target ($\rho_a = 8000$ kg m^{-3} instead of 3500) but assume $\beta = 10$.

For regolith covered rock (Fig. 3), the drag effect considered here falls far below the diurnal Yarkovsky effect, near the seasonal. The lower thermal conductivity of the regolith-covered body enhances the Yarkovsky effect by increasing the day-night temperature difference.

Since small asteroids tend to be more quickly rotating and have smaller gravitational attractions, it has been argued that they are unlikely to have substantial regolith (Farinella et al., 1998). If this is correct and meter-class stony asteroids do not usually have regolith coatings, then meteoroid impact drag will compete with

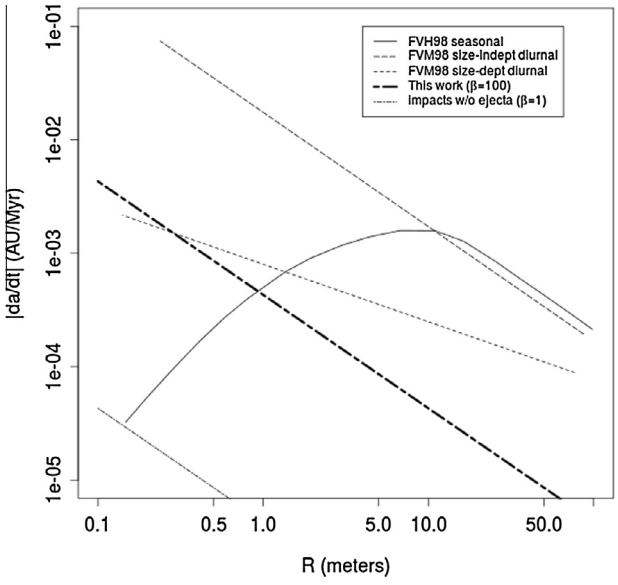

Fig. 1. The maximum semimajor axis drift for bare basalt fragment at 2 AU. The curves for the seasonal and diurnal Yarkovsky effect, either with a size-independent spin period of 5 h or with spin rate proportional to $1/R$ are adapted from Farinella et al. (1998) Fig. 1.

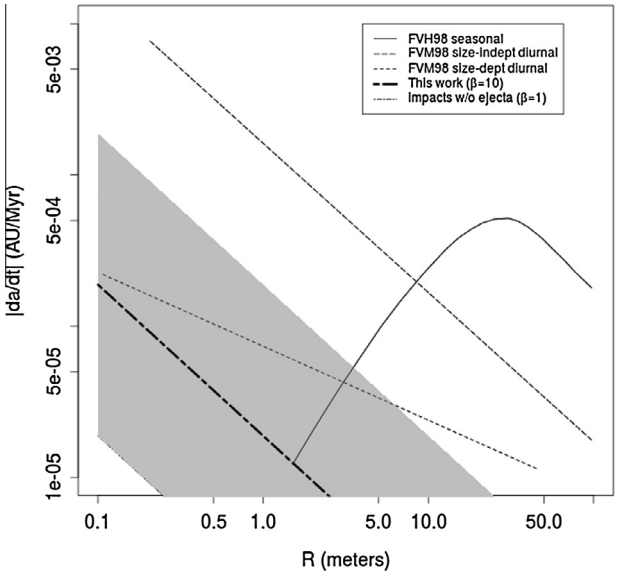

Fig. 2. The maximum semimajor axis drift for bare iron fragment at 2 AU. The curves for the seasonal and diurnal Yarkovsky effect, either with a size-independent spin period of 5 h or with spin rate proportional to $1/R$ are adapted from Farinella et al. (1998) Fig. 3. A gray region indicates a factor of 10 around the meteoroid drag line, indicating the high level of uncertainty in this value.

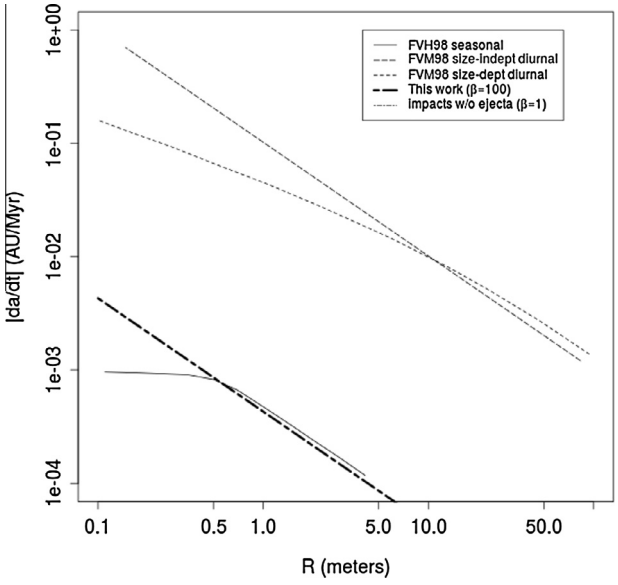

Fig. 3. The maximum semimajor axis drift for a regolith-covered fragment at 2 AU. The curves for the seasonal and diurnal Yarkovsky effect, either with a size-independent spin period of 5 h or with spin rate proportional to $1/R$ are adapted from Farinella et al. (1998) Fig. 4.

Yarkovsky effect in importance for stony meteorite delivery to Earth. It will be less important in the delivery of regolith-covered bodies or iron asteroids.

3.4. Uncertainties

Many unknowns cloud the true importance of the effect of meteoroid impact drag. Microcratering experiments seldom reach impact speeds beyond 10 km s^{-1} due to the difficulty in accelerating the projectile. The meteoroid impacts considered here are much faster: does this increase or decrease the effective drag force? The meteoroid environment at the asteroid belt is uncertain,

and our estimate could easily be off by an order of magnitude. Even the meteoroid flux at Earth is not particularly well known. An earlier measurement of the flux of impactors by (Grün et al., 1985) had a number three times smaller than that of Love and Brownlee (1993). Working in the opposite direction, the slope of the differential mass distribution of meteoroids near the Earth is close to −2 (Blaauw et al., 2011; Campbell-Brown and Braid, 2011). Values less than −2 imply most of the mass is in the smallest particles (which is what we have assumed here) while a value of precisely −2 means that each decade of mass contributes equally. The proximity of the slope to −2 means that our choice of typical impactor mass may be an underestimate, in which case the real effect would be larger than our prediction.

Our model of the meteoroid environment in the asteroid belt is based on an extrapolation of that measured at Earth. Though there are very few measurements of the meteoroid environment at the main belt, some spacecraft have done so, though at sizes far below those of interest here. These results have been synthesized by Divine (1993) and refined by later researchers (e.g. Matney and Kessler, 1996). Our results are consistent with Divine's finding that a retrograde meteor component is needed in the asteroid belt to match measurements. However our fluxes are over an order of magnitude higher than his, and this is worth further discussion.

A detailed comparison is not performed here because of the complexity in reproducing Divine's results in detail. Matney and Kessler (1996) work through Divine's model and find that he uses non-standard probability distributions which are not documented in the original paper itself. These appear to be internally consistent but make comparison with other references difficult and fraught with the potential for error. However, a simple order of magnitude comparison can be made by examining the figures in Divine's paper.

Our interest is in retrograde meteors, which in the Divine model are represented in only one of the five components, namely the 'halo' component. Divine's Fig. 9, which shows cumulative numbers below a certain size as a function of heliocentric distance, can be used for a crude estimate. Our size limit is 1.5×10^{-5} g, while Divine plots curves for 10^{-4} g and 10^{-9} g. Interpolating at 3.5 AU, the concentration is about 3×10^{-14} m^{-3} which for corresponds to a flux of 10^{-9} m^{-2} s^{-1}. Our number is 2×10^{-8} m^{-2} s^{-1} at this distance which is a factor of 20 higher than Divine's prediction.

As a result, the Divine model predicts that the meteoroid drag effect described here might be much weaker than we have assumed in the discussion above. Though certainly more information is needed about the meteoroid environment at the asteroid belt, we prefer our determination of the meteoroid flux because it is based on a much smaller extrapolation than Divine's model. Our model is based on large number statistics measured at Earth at the sizes of interest, extrapolated a factor of three in distance to the asteroid belt. The Divine model is based on measurements taken in the asteroid belt, but with small number statistics and extrapolated by many orders of magnitude in mass to the size range of relevance here.

The Divine model's 'halo' model component is designed to fit the Pioneer and Ulysses data that cannot be matched with the other components. Some retrograde component was deemed necessary, and this is consistent with the meteoroid environment assumed here. But the Pioneer detector (Humes, 1980) measured small particles, typically 10^{-8} to 10^{-9} g, and very few. Pioneer 10 saw only 95 particles from Earth to 18 AU, while Pioneer 11 saw 55 from Earth to Saturn. Particles at 1.5×10^{-5} g (which is what we consider here) would have been too infrequent to have been detected. A similar argument applies to Ulysses which was capable of detecting a 10^{-13} g meteoroid but only detected 72 impacts between 1.03 and 5.17 AU on its outward bound leg (Grün et al., 1992). Divine extrapolates in his model from the measured smaller sizes to larger ones, over several orders of magnitude in mass. We extrapolate the environment measured at Earth in the size range of interest out to the asteroid belt (a factor of 3 in distance), a less risky process in our opinion. Nonetheless, the question of the importance of meteoroid drag in the asteroid belt won't be answered until better models of the meteoroid environment there are available.

The physics of microcratering on an asteroidal target provide other unknowns in terms of shape, composition and strength. For example, impacts typically eject material on average perpendicular to the normal of the surface except for the most oblique impacts (Vedder, 1971). This effect will lessen the back-reaction when the impact takes place on the limb of the target. On the other hand, hypervelocity impactors are known to produce secondary craters (Hörz et al., 1971), which may themselves release more mass, particularly if the impact takes place into a pre-existing concavity such as a crater. The breakage of edges and the release of unconsolidated material, the rupture of the body or pieces thereof (Gault et al., 1972) may also serve to increase the total momentum released by an impact.

3.5. Rotational state of the parent

The two varieties of the Yarkovsky effect, the traditional or 'diurnal' (Öpik, 1951; Peterson, 1976) and 'seasonal' (Rubincam, 1995; Rubincam, 1998) affect asteroid orbits differently. The diurnal effect can either increase or decrease a depending on the body's rotation state. The seasonal effect always acts to decrease the semi-major axis, though its magnitude also depends on the orientation of the asteroid's rotation pole relative to the Sun. The impact drag effect considered here is independent of the rotation state of the asteroid. However meteoroid impacts can re-orient the spin of the asteroid or induce tumbling and thus may play an important indirect role in the Yarkovsky effect itself.

The rotational effect of impacts onto asteroid surfaces is a randomization of the pole, and each impact has an equal chance to increase or decrease the spin rate. These effects apply regardless of asteroid size, though smaller asteroids are more strongly affected by a single impact than larger ones. Studies which find faster spin rates for smaller asteroids (e.g. Harris and Pravec, 2006) are consistent with our discussion here. We do not expect that impacts would produce any net trends in asteroid pole orientations with size.

We do note here that the excess of retrograde versus prograde spins that has been found in the NEA population (La Spina et al., 2004) is more consistent with Yarkovsky-dominated injection than the meteoroid drag discussed here, as this latter effect is insensitive to the rotation state of the target. Though not all the asteroids in the sample of La Spina et al. (2004) are identified by name, it appears they are bodies which are mostly 1–10 km in diameter (Kaasalainen et al., 2004) and so do not reach the sizes where we expect impact drag to dominate. If the spin states of meter-class bodies could be measured then they might provide a valuable test for distinguishing these two effects but observational testing will have to await technological improvements.

The order-of-magnitude assumption that is usually made in calculating the time between pole reorientations involves equating the rotational angular momentum of the asteroid to that imparted by the impactor to determine the minimum size needed (at some typical encounter velocity) to perform such a reorientation. A knowledge of the size distribution of the impactors then allows the frequency of such impacts to be estimated. However, the momentum carried by the ejecta also comes into play here: the rotational momentum imparted by the impactor is not just its own momentum times the radius of the target, but β times as much. Though many poorly-understood effects (e.g. asteroid

composition, shape, internal cohesiveness, the direction of debris ejection under impacts near the limb of the asteroid, *etc.*) would come into play in a detailed calculation, to first order the angular momentum transferred to the asteroid is increased by a factor of β over that usually assumed, which means that a particle of only β^{-1} of the mass or $\beta^{-1/3}$ the radius can effect the same rotational change. For $\beta \sim 100$, this translates into a decrease by a factor of $100^{1/3} \approx 4.6$ in radius. Given that the cumulative distribution of impactor sizes goes something like $R^{-5/2}$ (Dohnanyi, 1969) this translates to reorientation events occurring $\beta^{5/6} = 100^{5/6} \approx 46$ times more frequently.

Thus, the net effectiveness of the diurnal variant of the Yarkovsky effect in particular may be considerably reduced. Meteoroid impacts do not reduce the height of the Yarkovsky curves in Figs. 1–3, instead they cause the sign of the effect to change more frequently, that is, if tumbling is not produced instead. If the distance between the asteroid and the resonance is Δa, then the escape process will be of the nature of a random walk if the time between pole reorientations τ_{rot} times $\dot{a}$ is greater than Δa. The more frequently reorientations occur, the more asteroids will be in the random-walk regime. Such asteroids will have a net Yarkovsky drift that proceeds at a rate that is diminished by roughly one over square root of $\beta^{5/6}$ ($\sim 0.15 \sim 1/7$). This additional factor may mean the smaller but consistently directed effect of meteoroid impacts can compete with the diurnal Yarkovsky effect at even larger sizes than Figs. 1–3 would imply.

4. The YORP effect

The Yarkovsky–O'Keefe–Radzievskii–Paddack (YORP) effect can change an asteroid's spin through the uneven re-radiation of thermal photons. Meteoroid impacts onto an asteroidal surface can change the rotation rate of the target at rates which are below (but perhaps uncomfortably close to) those currently being reported for YORP detections in near-Earth asteroids.

The angular momentum transferred to the target in a single impact is roughly $\Delta L = \beta m v R$, while the target's initial angular momentum is $L = I\omega$ where I is its moment of inertia (here taken to be that of a sphere $I = \frac{2}{5}MR^2$) and ω is its angular rate of rotation, related to its period P through $P = 2\pi/\omega$. The fractional change in angular momentum from a single impact is

$$\frac{\Delta L}{L} = \frac{\beta m v R}{\omega\left(\frac{2}{5}MR^2\right)} = \frac{15\beta m v P}{16\pi^2 \rho_a R^4} \tag{16}$$

If we ignore the small change in the moment of inertia of the target under the erosive effect of the impacts, then change in angular momentum produces a concomitant change in the rotation rate of the target, $\Delta\omega/\omega \approx \Delta L/L$. However, since individual impacts occur randomly on the surface, they are as likely to speed up the rotation as slow it down.

Let us consider the first reported detection of the YORP effect by Lowry et al. (2007) and Taylor et al. (2007). The asteroid (54509) YORP was observed to have its period decreasing at a fractional rate of -1.7×10^{-6} per year. Assuming a mean radius of 57 m and a rotation period of 730 s for this asteroid, Eq. (16) becomes

$$\frac{\Delta\omega}{\omega} \approx 1.6 \times 10^{-10}\left(\frac{\beta}{100}\right)\left(\frac{\rho_a}{3500\,\mathrm{kg\,m^3}}\right)^{-1}\left(\frac{m}{1.5\times10^{-8}\,\mathrm{kg}}\right)\left(\frac{v}{60\,\mathrm{km\,s^{-1}}}\right) \tag{17}$$

so each impact affects the rotation rate by only one part in 10^{10}. Though minuscule, this is still much larger than the ratio of the impactor to target masses, which is of order 10^{-17}, and hints that meteoroids may be more effective at changing asteroid rotation rates than might initially be assumed. The difference arises from the high speed of the impactor relative to the rotation of the target: material even on the surface of (54509) YORP moves no quicker than about 0.5 m/s under rotation. The impactor contains 10^5 times as much momentum per unit mass as the target material, and momentum transport by ejecta multiplies it further.

The asteroid suffers an impact rate $sn\pi R^2$ which in this case results in approximately 5000 impacts per year on (54509) YORP. Assuming a simple one-dimensional random walk, the net fractional change in the period of order 10^{-8} per year. This is two orders of magnitude below the fractional change in period observed (-1.7×10^{-6} year^{-1}) and so small apex meteoroids do not affect the spin rate at the same level as YORP in this case.

A more recent determination of the YORP effect on asteroid 25143 Itokawa (Lowry et al., 2014) is also essentially unaffected by impacts from apex meteoroids. The rotation period is 12.14 h and its mean radius, 162 m (Scheeres et al., 2007). Despite its larger size, because of its slower rotation, the fractional change in angular momentum per impact is essentially the same, 1.5×10^{-11}. Itokawa's larger size means that the rate of impacts is slightly higher, approximately 4×10^4 per year, or a fractional change under a random walk of 3×10^{-8} year^{-1}. This is equivalent to a change in the rotation period of $\sim$1 ms over the course of one year, much less than the value reported by Lowry et al. (2014) of $\sim$45 ms year^{-1}.

The R^{-4} dependence of Eq. (16) implies that the rotation states of smaller asteroids are more susceptible to change by meteoroid impacts. If the random walk goes like the square root of number of impacts ($\propto R^2$), then the net effect should go like R^{-3}. This means that for the calculated effect of meteoroids of 1 ms year^{-1} to increase to 45 ms year^{-1}, a decrease in the asteroid size by only a factor of four is required. Thus the impact of high-speed apex meteoroids may significantly influence the rotation state (at least to the same degree as YORP) for asteroids smaller than a few tens of meters in size.

4.1. Single impacts

The relatively large effect that a single meteoroid can have raises the question of the smallest meteoroid impact that would produce a result comparable to that of YORP. Here we will examine the single impact required to create a fractional change in period of one part in 10^6 on 54509 YORP, comparable to that reported by Lowry et al. (2007) and Taylor et al. (2007) for the YORP effect.

Rearranging Eq. (16) gives a minimum impactor mass m needed to produce a given fractional change in rotation rate

$$m = \left(\frac{\Delta\omega}{\omega}\right)\frac{16\pi^2\rho_a R^4}{15\beta v P} \tag{18}$$

$$8.9\times10^{-5}\,\mathrm{kg}\left(\frac{\Delta\omega/\omega}{10^{-6}}\right)\left(\frac{\beta}{100}\right)^{-1}\left(\frac{\rho_a}{3500\,\mathrm{kg\,m^{-3}}}\right)\left(\frac{v}{60\,\mathrm{km/s}}\right)^{-1} \tag{19}$$

At 60 km s^{-1} impact speed, a fractional change in period of 10^{-6} could be generated by a single a 0.09 g meteoroid if $\beta = 100$. Such a particle is approximately 2 mm in radius at a density of 2500 kg m^{-3}.

The apex sources are rich in small particles but not in large ones. Though 2 mm radius particles certainly occur there, it is clear that in considering the relatively large asteroids examined here, impacts by larger particles will be more effective. We instead consider the effect of the sporadic meteoroid population as a whole, which has somewhat lower speeds but more larger particles.

The encounter velocities between typical sporadic meteoroids and the Earth are lower ($\sim$30 km s^{-1}, Campbell-Brown (2008)) than for apex meteoroids, and the value of β which scales roughly like v (Housen and Holsapple (2011, 2012)) is also reduced by a

factor of two. At this reduced speed and β, a mass of 0.72 g (Eq. (19)) is required to affect a spin change of one part in 10^6 in 54509 YORP.

To estimate the rate of such impacts, we use flux measurements at Earth. Using video recordings of meteors in Earth's atmosphere, Campbell-Brown and Braid (2011) found the total sporadic meteor flux to be 0.18 ± 0.04 km^{-2} h^{-1} (5×10^{-11} m^{-2} s^{-1}) down to a limiting mass of 2×10^{-6} kg and deduced a differential mass slope of -2.02 ± 0.02. A differential mass slope of near -2 implies that the cumulative impact rate is inversely proportional to the mass, and so the rates of impacts by meteoroids of at least 1.8×10^{-4} kg is approximately $(7.2 \times 10^{-4}/2 \times 10^{-6})^{-1}(5 \times 10^{-11}) = 1.4 \times 10^{-13}$ m^{-2} s^{-1}, or one every 22 years on (54509) YORP, which can be neglected considering that the data from Lowry et al. (2007) and Taylor et al. (2007) was collected over only 3–4 years.

The change in period reported for Itokawa is similar, 45 ms in 12.14 h or $\Delta P/P \sim 10^{-6}$. Though it is a larger body, owing to its slower rotation rate, an impactor of about the same mass as for the case of 54509 YORP is needed. Itokawa has a eight times the cross section though, and might see one such impact every 2–3 years, a rate which is arguably not entirely negligible given that the YORP data was collected over a span of 12 years (Lowry et al., 2014).

Though meteoroid impacts may have an important role to play, we are not asserting here that the spin changes attributed to YORP have actually been produced by meteoroid impacts, for two reasons. First, the observed changes in rotation are seen to be accelerating, which is more compatible with YORP than impacts (though admittedly a small number of impacts could conspire to look like a net acceleration in the short term). Secondly, the analysis above uses values of β deduced for bare rock. Itokawa at least is certainly regolith-covered (e.g. Fujiwara et al., 2006) which is likely to reduce β. If the impact rate is goes like the inverse of the impactor mass, then the rate of impacts capable of generating the required change in period goes roughly like β. A small reduction in β would then reduce the rate of impacts of concern to one every several years, which can be neglected. Nonetheless, we do conclude that the effect of impacts is at a level which demands some attention when sensitive measurements of asteroid spins are being made.

5. Other considerations

5.1. Other sporadic meteor sources and radiation pressure

There are six generally accepted sporadic meteoroid sources, that is, six broad inhomogeneities in the time-averaged meteoroid environment seen by the moving Earth (e.g. Stohl, 1986; Brown and Jones, 1995; Chau et al., 2007; Campbell-Brown, 2008). The north and south apex sources have been the basis of the analysis so far. Two others are the north and south toroidal sources, which also arrive at the Earth from the direction roughly opposite its motion but at higher ecliptic latitudes. These may contribute to the drag force considered here but are generally weaker than the apex sources and have been neglected here. The two remaining sources are the helion and antihelion sources, consisting of particles on high-eccentricity orbits which hit the Earth from the directions of the Sun and of opposition respectively. These particles may create a small radial force component on asteroids but have been ignored here so far because the helion and antihelion sources have roughly equal strengths, and so the net force from them will average out. Though it is perhaps worth noting that the strengths are not precisely equal, the antihelion source may in fact be stronger but probably only by about 20–30% (see Wiegert et al. (2009) and references therein.).

One might wonder if the helion or antihelion meteoroid sources, owing to the radial nature of the forces they create, could confound measurements of the radiation pressure on small asteroids, which have been used to determine their densities in particular cases (Micheli et al., 2012, 2013, 2014). We can show that the meteoroid drag as considered here is much smaller than radiation pressure near the Earth. Even if we ignore the opposing nature of the helion and antihelion sources and assume that one or the other constitutes all of the meteoroid impacts considered in Eq. (1), the effect is less than radiation pressure. Adopting the expression of Burns et al. (1979) for the ratio of radiation pressure to solar gravity and combining that with Eq. (1) yields a ratio of radiation to meteoroid-derived accelerations β_m of

$$\beta_m = \frac{L_\odot Q_{PR}}{4\pi c s n m v r^2 \beta} \sim 7 \times 10^3 \tag{20}$$

where $L_\odot$ is the solar luminosity, Q_{PR} is a radiation absorption coefficient we have taken to be unity, c is the speed of light, m and v are the impactor mass and velocities and r is the heliocentric distance. Here we have adopted $s = 0.5$ and an impact velocity $v = 30$ km s^{-1} more appropriate for the helion and anti-helion sources but this makes little difference; the effect of meteoroid drag is much smaller than radiation pressure under all reasonable conditions.

5.2. Erosion rates

The large amounts of ejecta produced by meteoroid impacts also contribute to the erosion of the target body. The 1.5×10^{-8} kg impactor considered here releases 3.1×10^{-4} kg of ejecta if $N = 2 \times 10^4$. At the Earth's orbit this translates into a rough survival time τ against erosion of a stony body

$$\tau \sim 16\ \mathrm{Myr}\left(\frac{\rho_a}{3500\ \mathrm{kg\ m^{-3}}}\right)\left(\frac{R}{1\ \mathrm{m}}\right) \tag{21}$$

where this simple expression is an upper limit, as it ignores the decreasing impact rate as the target size decreases. This time is comparable to the dynamical lifetimes (10 Myr, Gladman et al., 1997, 2000) of near-Earth asteroids and so the high levels of ejecta production assumed here do not conflict with reality on this basis. The high erosion rates proposed here are also consistent with cosmic ray exposure ages of meteorites. The cosmic ray exposure (CRE) ages of stony meteorites rarely exceed 100 Myr (Herzog, 2005) which can be accommodated in Eq. (21) by a parent body of 10 m in size. This is broadly consistent with more detailed consideration of the effect of erosion on meteorite CRE ages provided by Rubincam (2015).

6. Conclusions

We have discussed the effect of the meteoroid environment on small asteroids. It was argued that ejecta production amplifies the net effect of such impacts into regolith by an order of magnitude, and by up to two orders of magnitude into bare rock surfaces. Iron asteroids are also affected though to a more limited degree. Careful examination of the physics of hypervelocity impacts will be needed to determine the exact magnitude of the effect and its broader role in asteroid evolution.

The instantaneous value of the net drag produced by the apex meteoroids is found to exceed that of both the diurnal and seasonal variants of Yarkovsky effect at sizes below one meter if bodies at these sizes are bare rock. This is perhaps to be expected for smaller bodies which typically have faster spins, but remains to be confirmed. At larger sizes the seasonal Yarkovsky effect is more important. Drag against the meteoroid environment is independent of thermal or rotational properties of individual asteroids, though not their densities. Independence from the rotation state means that the meteoroid environment acts consistently as a drag and

cannot increase an asteroid's semimajor axis. Impacts also serve to reorient the spin axis of the target or induce tumbling, and thus can decrease the net effectiveness of Yarkovsky drift.

As a result, meteoroid drag is an important factor in the delivery of meter-class asteroids and below to main belt resonant escape hatches, where some are transferred to near-Earth space. As meter-class bodies are the smallest that can survive atmospheric entry, meteoroid drag may prove to be an important mechanism for delivering meteorites to Earth. Meter-class asteroids are also of interest as potential targets of the Asteroid Redirect Mission (e.g. Brophy et al., 2012), and the first few NEAs at these sizes are now being characterized. Recent detailed studies of small NEAs (2009 BD, 3–4 m diameter (Mommert et al., 2014, and 2011 MD, 6 m diameter (Mommert et al., 2014)) both show the effects of a weak drag force. It will be interesting to see if such small bodies show any distinct characteristics which can be attributed to their delivery mechanism, though this will not be easy to determine.

The meteoroid impacts have the potential to confuse measurements of the YORP effect. Here the effect is primarily due to larger (centimeter) sized particles from the general sporadic meteoroid population. However we conclude that impacts have probably not clouded recent measurements of YORP among the near-Earth asteroid population, though it will be an important consideration when measurements of smaller (10 m class) bodies are made. In fact, high precision asteroid spin measurements may be sensitive enough to measure the effect of meteoroid impacts on spin states.

The effects of meteoroid impacts on the dynamics of small asteroids remains to be worked out in detail. If the momentum transport by ejecta proposed here correctly represents real meteoroid–asteroid collisions, then meteoroid impacts may prove to be as important as radiative effects in the dynamical evolution of small asteroids and the transport of meteorites to Earth.

Acknowledgments

We thank David Rubincam and Davide Farnocchia for valuable comments that much improved this paper. This work was performed in part with funding from the Natural Sciences and Engineering Research Council of Canada.

References

Blaauw, R.C., Campbell-Brown, M.D., Weryk, R.J., 2011. Mass distribution indices of sporadic meteors using radar data. Mon. Not. R. Astron. Soc. 412, 2033–2039. http://dx.doi.org/10.1111/j.1365-2966.2010.18038.x.

Braslau, D., 1970. Partitioning of energy in hypervelocity impact against loose sand targets. J. Geophys. Res. 75, 3987–3999. http://dx.doi.org/10.1029/JB075i020p03987.

Brophy, J., Culick, F., Friedman, F., et al., 2012. Asteroid Retrieval Feasibility Study. Technical Report Keck Institute for Space Studies.

Brown, P., Jones, J., 1995. A determination of the strengths of the sporadic radio-meteor sources. Earth Moon Planets 68, 223–245. http://dx.doi.org/10.1007/BF00671512.

Burns, J.A., Lamy, P.L., Soter, S., 1979. Radiation forces on small particles in the Solar System. Icarus 40, 1–48. http://dx.doi.org/10.1016/0019-1035(79)90050-2.

Campbell-Brown, M.D., 2008. High resolution radiant distribution and orbits of sporadic radar meteoroids. Icarus 196, 144–163. http://dx.doi.org/10.1016/j.icarus.2008.02.022.

Campbell-Brown, M.D., Braid, D., 2011. Video meteor fluxes. In: Cooke, W.J., Moser, D.E., Hardin, B.F., Janches, D. (Eds.), Meteoroids: The Smallest Solar System Bodies, pp. 304–312.

Carter, L.M., Campbell, D.B., Nolan, M.C., 2006. Regolith cover on near-Earth asteroids: Radar polarimetric imaging and analysis. In: AAS/Division for Planetary Sciences Meeting Abstracts #38. Bulletin of the American Astronomical Society, vol. 38, p. 621.

Chau, J.L., Woodman, R.F., 2004. Observations of meteor head-echoes using the Jicamaraca 50 mHz radar in interferometer mode. Atmos. Chem. Phys. 4, 511–521.

Chau, J.L., Woodman, R.F., Galindo, F., 2007. Sporadic meteor sources as observed by the Jicamarca high-power large-aperture VHF radar. Icarus 188, 162–174. http://dx.doi.org/10.1016/j.icarus.2006.11.006.

Cheng, A.F., 2002. Near Earth asteroid rendezvous: Mission summary. Asteroids III, 351–366.

Comerford, M.F., 1967. Comparative erosion rates of stone and iron meteorites under small-particle bombardment. Geochim. Cosmochim. Acta 31, 1457–1471.

Delbó, M., Harris, A.W., Binzel, R.P., Pravec, P., Davies, J.K., 2003. Keck observations of near-Earth asteroids in the thermal infrared. Icarus 166, 116–130. http://dx.doi.org/10.1016/j.icarus.2003.07.002.

Divine, N., 1993. Five populations of interplanetary meteoroids. J. Geophys. Res. 98, 17029–17048. http://dx.doi.org/10.1029/93JE01203.

Dohnanyi, J.S., 1969. Collisional model of asteroids and their debris. J. Geophys. Res. 74, 2531–2554.

Farinella, P., Vokrouhlicky, D., Hartmann, W.K., 1998. Meteorite delivery via Yarkovsky orbital drift. Icarus 132, 378–387. http://dx.doi.org/10.1006/icar.1997.5872.

Fechtig, H., Gault, D.E., Neukum, G., Schneider, E., 1972. Laboratory simulation of lunar craters. Naturwissenschaften 59, 151–157. http://dx.doi.org/10.1007/BF00637353.

Fujiwara, A. et al., 2006. The rubble-pile Asteroid Itokawa as observed by Hayabusa. Science 312, 1330–1334. http://dx.doi.org/10.1126/science.1125841.

Galligan, D.P., Baggaley, W.J., 2004. The orbital distribution of radar-detected meteoroids of the Solar System dust cloud. Mon. Not. R. Astron. Soc. 353, 422–446. http://dx.doi.org/10.1111/j.1365-2966.2004.08078.x.

Gault, D.E., 1973. Displaced mass, depth, diameter, and effects of oblique trajectories for impact craters formed in dense crystalline rocks. Moon 6, 32–44. http://dx.doi.org/10.1007/BF02630651.

Gault, D.E., Hörz, F., Hartung, J.B., 1972. Effects of microcratering on the lunar surface. In: Metzger, A.E., Trombka, J.I., Peterson, L.E., Reedy, R.C., Arnold, J.R. (Eds.), Proc. Lunar Sci. Conf., vol. 3, p. 2713.

Gladman, B.J. et al., 1997. Dynamical lifetimes of objects injected into asteroid belt resonances. Science 277, 197–201.

Gladman, B., Michel, P., Froeschlé, C., 2000. The near-Earth object population. Icarus 146, 176–189. http://dx.doi.org/10.1006/icar.2000.6391.

Grün, E. et al., 1992. Galileo and ULYSSES dust measurements – From Venus to Jupiter. Geophys. Res. Lett. 19, 1311–1314. http://dx.doi.org/10.1029/92GL00629.

Grün, E., Zook, H.A., Fechtig, H., Giese, R.H., 1985. Collisional balance of the meteoritic complex. Icarus 62, 244–272. http://dx.doi.org/10.1016/0019-1035(85)90121-6.

Harris, A.W., Pravec, P., 2006. Rotational properties of asteroids, comets and TNOs. In: Daniela, L., Sylvio Ferraz, M., Angel, F.J. (Eds.), Asteroids, Comets, Meteors. IAU Symposium, vol. 229, pp. 439–447. doi: http://dx.doi.org/10.1017/S1743921305006903.

Hartmann, W.K., 1983. Energy partitioning in impacts into regolith-like powders. Lunar Planet. Sci., vol. 14, pp. 281–282.

Hartmann, W.K., 1985. Impact experiments. I – Ejecta velocity distributions and related results from regolith targets. Icarus 63, 69–98. http://dx.doi.org/10.1016/0019-1035(85)90021-1.

Hatch, P., Wiegert, P.A., 2015. On the rotation rates and axis ratios of the smallest known near-Earth asteroids – the potential targets of the Asteroid Redirect Mission. Planet. Space Sci., in press.

Herzog, G.F., 2005. Cosmic-ray exposure ages of meteorites. In: Davis, A.M., Holland, H.D., Turekian, K.K. (Eds.), Meteorites, Comets and Planets: Treatise on Geochemistry, vol. 1. Elsevier B.V., Amsterdam, The Netherlands, p. 347. ISBN 0-08-044720-1.

Hörz, F., Hartung, J.B., Gault, D.E., 1971. Micrometeorite craters on lunar rock surfaces. J. Geophys. Res. 76, 5770–5798. http://dx.doi.org/10.1029/JB076i023p05770.

Housen, K.R., Holsapple, K.A., 2011. Momentum transfer in hypervelocity collisions. Lunar Planet. Sci., vol. 42, p. 2363.

Housen, K.R., Holsapple, K.A., 2012. Deflecting asteroids by impacts: What is beta? Lunar Planet. Sci., vol. 43, p. 2539.

Humes, D.H., 1980. Results of Pioneer 10 and 11 meteoroid experiments – Interplanetary and near-Saturn. J. Geophys. Res. 85, 5841–5852. http://dx.doi.org/10.1029/JA085iA11p05841.

Hunt, S.M., Oppenheim, M., Close, S., Brown, P.G., McKeen, F., Minardi, M., 2004. Determination of the meteoroid velocity distribution at the Earth using high-gain radar. Icarus 168, 34–42. http://dx.doi.org/10.1016/j.icarus.2003.08.006.

Janches, D., Nolan, M.C., Meisel, D.D., Mathews, J.D., Zhou, Q.H., Moser, D.E., 2003. On the geocentric micrometeor velocity distribution. J. Geophys. Res. (Space Phys.) 108, 1222–1235. http://dx.doi.org/10.1029/2002JA009789.

Jones, J., Brown, P., 1993. Sporadic meteor radiant distributions – Orbital survey results. Mon. Not. R. Astron. Soc. 265, 524–532.

Kaasalainen, M. et al., 2004. Photometry and models of eight near-Earth asteroids. Icarus 167, 178–196. http://dx.doi.org/10.1016/j.icarus.2003.09.012.

La Spina, A., Paolicchi, P., Kryszczyńska, A., Pravec, P., 2004. Retrograde spins of near-Earth asteroids from the Yarkovsky effect. Nature 428, 400–401. http://dx.doi.org/10.1038/nature02411.

Love, S.G., Brownlee, D.E., 1993. A direct measurement of the terrestrial mass accretion rate of cosmic dust. Science 262, 550–553.

Lowry, S.C. et al., 2007. Direct detection of the asteroidal YORP effect. Science 316, 272–274. http://dx.doi.org/10.1126/science.1139040.

Lowry, S.C. et al., 2014. The internal structure of Asteroid (25143) Itokawa as revealed by detection of YORP spin-up. Astron. Astrophys. 562, A48–A56. http://dx.doi.org/10.1051/0004-6361/201322602.

Matney, M.J., Kessler, D.J., 1996. A reformulation of Divine's interplanetary model. In: Gustafson, B.A.S., Hanner, M.S. (Eds.), IAU Colloq. 150: Physics, Chemistry, and Dynamics of Interplanetary Dust. Astronomical Society of the Pacific Conference Series, vol. 104, p. 15.

Micheli, M., Tholen, D.J., Elliott, G.T., 2012. Detection of radiation pressure acting on 2009 BD. New Astron. 17, 446–452. http://dx.doi.org/10.1016/j.newast.2011.11.008, arXiv:1106.0564.
Micheli, M., Tholen, D.J., Elliott, G.T., 2013. 2012 LA, an optimal astrometric target for radiation pressure detection. Icarus 226, 251–255. http://dx.doi.org/10.1016/j.icarus.2013.05.032.
Micheli, M., Tholen, D.J., Elliott, G.T., 2014. Radiation pressure detection and density estimate for 2011 MD. Astrophys. J. 788, L1-5. http://dx.doi.org/10.1088/2041-8205/788/1/L1, arXiv:1403.6033.
Mommert, M. et al., 2014. Constraining the physical properties of near-Earth object 2009 BD. ApJ 786, 148–156.
Öpik, E., 1951. Collision probability with the planets and the distribution of planetary matter. Proc. R. Irish Acad. Sect. A 54, 165–199.
Peterson, C., 1976. A source mechanism for meteorites controlled by the Yarkovsky effect. Icarus 29, 91–111. http://dx.doi.org/10.1016/0019-1035(76)90105-6.
Rabinowitz, D.L., 1993. The size distribution of Earth-approaching asteroids. Astrophys. J. 407, 412–427.
Rabinowitz, D.L. et al., 1993. Evidence for a near-Earth asteroid belt. Nature 363, 704–706. http://dx.doi.org/10.1038/363704a0.
Roy, A.E., 1978. Orbital Motion. Adam Hilger Ltd., Bristol.
Rubincam, D.P., 1995. Asteroid orbit evolution due to thermal drag. J. Geophys. Res. 100, 1585–1594. http://dx.doi.org/10.1029/94JE02411.
Rubincam, D.P., 1998. Yarkovsky thermal drag on small asteroids and Mars–Earth delivery. J. Geophys. Res. 103, 1725–1732. http://dx.doi.org/10.1029/97JE03034.
Rubincam, D.P., 2015. Space erosion and cosmic ray exposure ages of stony meteorites. Icarus 245, 112–121.
Saito, J. et al., 2006. Detailed images of Asteroid 25143 Itokawa from Hayabusa. Science 312, 1341–1344. http://dx.doi.org/10.1126/science.1125722.
Sato, T., Nakamura, T., Nishimura, K., 2000. Orbit determination of meteors using the MU radar. IEICE Trans. Commun. E83-B (9), 1990–1995.
Schaeffer, O.A., Nagel, K., Neukum, G., Fechtig, H., 1979. Effects of micrometeorite bombardment on cosmic ray ages of stony and iron meteorites: Evidence for a long term temporal change in cosmic ray intensity. Lunar Planet. Sci., vol. 10, pp. 1061–1062.
Scheeres, D.J., Abe, M., Yoshikawa, M., Nakamura, R., Gaskell, R.W., Abell, P.A., 2007. The effect of YORP on Itokawa. Icarus 188, 425–429. http://dx.doi.org/10.1016/j.icarus.2006.12.014.
Stohl, J., 1986. Seasonal variation in the radiant distribution of meteors. In: Kresak, L., Millman, P.M. (Eds.), Physics and Dynamics of Meteors. IAU Symposium, vol. 33, pp. 298–303.
Taylor, A.D., 1995. The Harvard radio meteor project velocity distribution reappraised. Icarus 116, 154–158. http://dx.doi.org/10.1006/icar.1995.1117.
Taylor, P.A. et al., 2007. Spin rate of Asteroid (54509) 2000 PH5 increasing due to the YORP effect. Science 316, 274–277. http://dx.doi.org/10.1126/science.1139038.
Tedeschi, W.J., Remo, J.L., Schulze, J.F., Young, R.P., 1995. Experimental hypervelocity impact effects on simulated planetesimal materials. Int. J. Impact Eng. 17, 837–848.
Vedder, J.F., 1971. Microcraters in glass and minerals. Earth Planet. Sci. Lett. 11, 291–296. http://dx.doi.org/10.1016/0012-821X(71)90182-8.
Vedder, J.F., 1972. Craters formed in mineral dust by hypervelocity microparticles. J. Geophys. Res. 77, 4304–4309. http://dx.doi.org/10.1029/JB077i023p04304.
Weidenschilling, S.J., Jackson, A.A., 1993. Orbital resonances and Poynting–Robertson drag. Icarus 104, 244–254.
Wiegert, P., Vaubaillon, J., Campbell-Brown, M., 2009. A dynamical model of the sporadic meteoroid complex. Icarus 201, 295–310. http://dx.doi.org/10.1016/j.icarus.2008.12.030.
Yanagisawa, M., Hasegawa, S., 2000. Momentum transfer in oblique impacts: Implications for asteroid rotations. Icarus 146, 270–288. http://dx.doi.org/10.1006/icar.2000.6389.